JACS
JOURNAL OF THE AMERICAN CHEMICAL SOCIETY
Article
pubs.acs.org/JACS

General Insights into Structural Evolution of Layered Double Hydroxide: Underlying Aspects in Topochemical Transformation from Brucite to Layered Double Hydroxide

Renzhi Ma,* Jianbo Liang, Xiaohe Liu, and Takayoshi Sasaki

International Center for Materials Nanoarchitectonics (WPI-MANA), National Institute for Materials Science (NIMS), 1-1 Namiki, Tsukuba, Ibaraki 305-0044, Japan

ABSTRACT: The topochemical transformation from transition-metal brucite hydroxide ($Co_{1-x}Fe_x(OH)_2$, $Co(OH)_2$, $Co_{1-x}Ni_x(OH)_2$) to corresponding (Co^{2+}–(Co^{3+})–Fe^{3+}, Co^{2+}–(Ni^{2+})–Co^{3+}) LDH under oxidizing halogen agents (iodine, bromine) exhibits different staging phenomena depending on the metallic composition/ratio in starting brucite. A plausible charge hopping mechanism based on valence interchange between redoxable charge center (Fe^{3+}/Co^{3+}) and neighboring divalent sites in the host sheet is proposed to understand the restoration of electron donor sites at the interface between brucite crystallites and halogen agents, which ensures a continual oxidative reaction, and a staged intercalation/diffusion of *in situ* reduced halide anions into the interlayer gallery commensurate with the host charge propagation. The discussion on the correlation between staging product and metallic composition/ratio offers a general perspective and new insights into M^{2+}/M^{3+} ratio and cation ordering, host layer charge, and phase evolution in LDH structure.

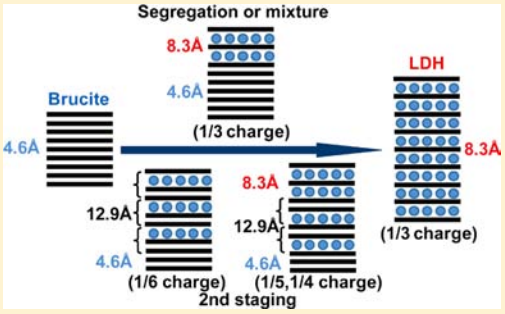

INTRODUCTION

The most basic and simplest form of layered hydroxide is a brucite-type structure ($M^{2+}(OH)_2$), in which neutral host layers (sheets, slabs) are composed of M^{2+}-centered octahedra coordinated with six hydroxyl groups (OH^-) locating in the vertices whereas each OH^- is surrounded by three metal cations. The individual sheets are held to one another by van der Waals force and hydrogen bonds. Other closely related phases may be perceived as derivates from compositional changes and corresponding structural modifications to the brucite prototype. For example, if trivalent cations (M^{3+}) isomorphically replace some of the M^{2+} sites, inducing excessive positive electric charge to the host sheets, the structure needs to intercalate chemical species bearing compatible counter charges, i.e., anions. This results in an expansion in the dimension along layer stacking direction, whereas the structure framework is still maintained. Such an evolved structure is well-known as layered double hydroxide (LDH), which may be expressed by a generic formula of $[M^{2+}_{1-x}M^{3+}_x(OH)_2]^{x+}[A^{n-}_{x/n}]^{x-}\cdot mH_2O$ (M^{2+} and M^{3+} represent di- and trivalent metal cations, respectively; A^{n-} represents charge-balancing *n*-valent anion).[1−4] As a rare class of anion-exchangeable claylike materials, LDHs and some analogous hydroxides are uniquely promising to combine both inorganic/organic anions and metal hydroxide layers, that could be readily developed into porous multimetal mixed oxide catalysts/supports,[5−7] and form variable nanometer-scale precursors, e.g., two-dimensional platelets[8] and one-dimensional nanocones,[9,10] which could be further exfoliated into functional unilamellar nanosheets.[11−13]

A diverse combination of M^{2+}–M^{3+} cations in LDH host sheets has been extensively pursued, and can be routinely attained through a convenient coprecipitation of corresponding di- and trivalent metal salts under an alkaline condition.[14−17] This in fact yields a large family of M^{2+}–M^{3+} LDHs (M^{2+} = Mg^{2+}, Fe^{2+}, Co^{2+}, Ni^{2+}, Zn^{2+}, etc., and M^{3+} = Al^{3+}, Fe^{3+}, Cr^{3+}, Ga^{3+}, etc.). Nevertheless, the research interest on LDH materials has been traditionally driven and dominated by M^{2+}–Al^{3+} category, particularly Mg^{2+}–Al^{3+}, partly due to the fact that hydrotalcite $Mg_6Al_2(OH)_{16}(CO_3)\cdot 4H_2O$ is a widely known anionic clay found in nature. In addition, the amphoteric feature of Al^{3+} also plays a very favorable role in promoting the precipitation and crystallization of M^{2+}–Al^{3+} LDHs. By virtue of this amphoteric feature, well-crystallized M^{2+}–Al^{3+} LDH crystallites have been readily synthesized via a homogeneous precipitation utilizing ammonia-releasing hydrolysis agents such as urea[18−23] or hexamethylenetetramine (HMT).[24,25] On the other hand, without the incorporation of amphoteric Al^{3+} into the host sheet, it is more difficult to synthesize LDH in a highly crystalline form. Consequently, non-Al^{3+} LDHs remain as a least explored category.

We have recently developed an innovative topochemical method for the synthesis of non-Al^{3+} LDHs, namely an oxidative intercalation based on redoxable transition-metal elements (Fe, Co, Ni), which exactly echoes the perceived structural transformation from brucite to LDH (Figure 1). Specifically, brucite-type hydroxides composed of divalent

Received: October 17, 2012
Published: November 8, 2012

ACS Publications © 2012 American Chemical Society

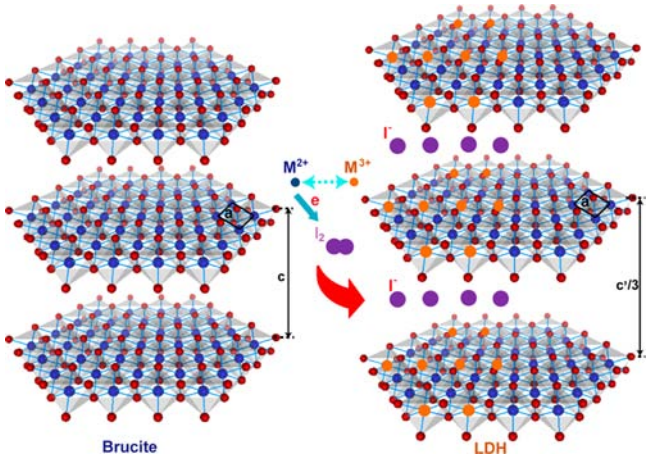

Figure 1. Schematic illustration of topochemical oxidative intercalation transforming brucite into LDH. A portion of M^{2+} cations (blue) in starting brucite, e.g., Fe^{2+}, are oxidized into M^{3+} (orange) by halogen agents (purple), e.g., I_2, whereas the reduced halogen anions (I^-) are intercalated between the sheets to prop up the gallery space and balance the layer charge, resulting in the formation of LDH. Red spheres represent hydroxyl (oxygen) groups. Labels a and c represent the basal and layer stacking axes of brucite and LDH.

transition-metal elements, such as $Co^{2+}_{1-x}Fe^{2+}_x(OH)_2$ ($0 < x \leq 1/3$), $Co^{2+}(OH)_2$, and $Co^{2+}_{1-x}Ni^{2+}_x(OH)_2$ ($0 < x \leq 1/2$), are partially oxidized and transformed into $Co^{2+}_{2/3}-(Co^{3+}_{1/3-x}-Fe^{3+}_x)$, $Co^{2+}_{2/3}-Co^{3+}_{1/3}$, and $(Co^{2+}_{1-3x/2}-Ni^{2+}_{3x/2})_{2/3}-Co^{3+}_{1/3}$ LDHs, respectively, intercalating charge-balancing counter-anions in the gallery.[26−29] As brucite-type transition-metal hydroxides with high crystallinity are easier to synthesize, such a topochemical transformation actually stands out as the only successful synthetic protocol currently available for LDH samples with all-transition-metal composition in a highly crystalline form comparable to their $M^{2+}-Al^{3+}$ analogues derived from homogeneous precipitation.

Central to the topochemical transformation are concomitant events of oxidizing a portion of divalent metal cations (Fe^{2+}, Co^{2+}) into a trivalent state (Fe^{3+}, Co^{3+}) by oxidizing agents such as iodine (I_2) or bromine (Br_2), introducing positive electric charge to the host sheets, whereas the halogen agents themselves are reduced into anions ($I^-(I_3^-)$, Br^-) and intercalated/diffused into the gallery. The key conditions for a successful transformation would be the choice of a halogen agent with suitable oxidation potential and effective accessibility/transfer of electrons from cations M^{2+} in the host sheet to the halogen agent. Therefore, charge propagation and redistribution within the host sheet, i.e., electron or hole hopping mobility in the brucite lattice, may be regarded as the most fundamental aspect of this important reaction.

Accompanying the development of positive electrical charge in brucite sheets, Coulombic repulsion would cause the sheets to separate, intercalating reduced halide anions into the gallery to serve as counter charge balancing species. Depending on the progress, a mixture of anion-intercalated LDH galleries and residual empty brucite ones, i.e., phase segregation, is expected. It thus creates an opportunity for an alternated stacking of LDH and brucite components in one crystallite, i.e., staging. As an interesting chemical process, staging phenomenon was commonly observed and intensively studied in the graphite intercalation compounds (GIC) as a consequence of the flexible nature of graphite sheets.[30,31] Staging in LDH was rare due to more rigid and thicker hydroxide layers. However, it was recently revealed that staging products could be derived from different interlayer contents or different orientation of the same anionic species compensating for host layer charge in LDH materials.[32−38] In our previous studies, evidence for a staging product in the transformation from $Co^{2+}-Fe^{2+}$ brucites to $Co^{2+}-Fe^{3+}$ LDHs, corresponding to an alternated stacking of I^--intercalated LDH slabs and residual brucite ones, also emerged.[26,29] The staging phenomenon can offer indispensable insights into the forming course of a LDH phase regarding host layer charge (M^{2+}/M^{3+} ratio) and anion intercalation, and thus, a comprehensive study is needed.

In a broader perspective, specific cation arrangement corresponding to the metallic composition/ratio in LDH host layers remains somewhat elusive,[39] due to the difficulty in precisely controlling the composition of LDH samples. It is generally accepted that a nominal value of x (host layer change) in $[M^{2+}_{1-x}M^{3+}_x(OH)_2]^{x+}[A^{n-}_{x/n}]^{x-}\cdot mH_2O$ is normally in the range $^1/_5-^1/_3$.[3] Larger or smaller values may cause the contaminant of hydroxide or hydrous oxides of a single metal. In addition, x outside this range requires extremely careful substantiation as some highly dispersed simple hydroxide phases are not easily to detect especially for low crystallinity or gel-like LDH samples, which is usually the case for coprecipitated samples. A recent report on cation ordering in coprecipitated $Mg^{2+}-Al^{3+}$ LDH, revealed by sophisticated multinuclear NMR spectroscopy, showed that the cations might be fully ordered for Mg^{2+}/Al^{3+} ratio of 2 ($x = ^1/_3$) and that at lower Al^{3+} content ($x = ^1/_4$, $^1/_5$), a nonrandom cation distribution on a microscopic level persists with no $Al^{3+}-Al^{3+}$ close contacts, i.e., coexisting neutral domains of brucite, and charged domains of LDH with Mg^{2+}/Al^{3+} ratio of 2.[40] However, for well-defined $M^{2+}-Al^{3+}$ LDH crystallites prepared from homogeneous precipitation, there is no success claim of M^{2+}/Al^{3+} cation ratio other than 2 ($x = ^1/_3$) except a rare case reported in hydrothermal homogeneous precipitation of $Ni^{2+}-Al^{3+}$ LDHs.[41] These contradictions reflect that a further understanding of M^{2+}/M^{3+} arrangement, more exactly cation ratio and ordering in LDH structure, is very necessary.

Unlike coprecipitation, the topochemical transformation was established on monodisperse, large-sized, and highly crystalline samples, an apparent advantage for the precise control on both the metallic composition and interlayer content, which would endow a unique insight into the thermodynamics and kinetics of LDH formation. In this work, on the basis of the experimental observations focusing on staging phenomena and the correlation with metallic composition/ratio in host sheets in the topochemical transformation from brucites to LDHs, a detailed scenario on plausible charge hopping mechanism and staged anion intercalation is presented, which is vital not only in portraying the underlying aspects of this particular oxidative intercalation reaction, but also in understanding the redox behavior in transition-metal hydroxides. More importantly, it sheds light on general principles governing the formation of a stable LDH structure when M^{2+}/M^{3+} cation ratio and ordering, host layer charge, and phase evolution are concerned.

■ EXPERIMENTAL SECTION

Highly crystalline hexagonal platelets of brucite hydroxides $Co(OH)_2$, $Co_{1-x}Fe_x(OH)_2$ ($x = ^1/_6$, $^1/_5$, $^1/_4$, $^1/_3$), and $Co^{2+}_{2/3}Ni^{2+}_{1/3}(OH)_2$ were synthesized via refluxing a dilute aqueous solution of divalent cobalt and/or ferrous (nickel) cations with HMT as hydrolysis agent under

nitrogen gas protection. Similar to our earlier reports,[26−29] all the synthesis yielded precipitates exhibiting a clear anisotropic stream under stirring, implying a large aspect ratio of the platelet products.

Designed amount of halogen agent (typically x mol iodine or bromine) was dissolved in 100 cm^3 of organic solvent (iodine in chloroform or bromine in acetonitrile). As-prepared brucite sample (typically 0.186 g, 2 mmol) was dispersed and magnetically stirred in the halogen solution at room temperature for 24 h for a stoichiometric reaction. For further oxidation, an excessive amount of halogen agents (>10 × x mol) was used, and the reaction was maintained from 24 h to 1 week. All reacted product were collected by filtering, and washing repeatedly with anhydrous ethanol until the filtrate appeared colorless.

X-ray diffraction (XRD) data were recorded on a Rigaku Rint-2200 diffractometer with monochromatic Cu Kα radiation (λ = 0.154 05 nm). Morphology of the synthesized products was examined using a JEOL JSM-6700F field emission scanning electron microscope (FE-SEM). The metallic contents in the samples were determined either by inductively coupled plasma (ICP) atomic emission spectroscopy (Seiko SPS1700HVR) after dissolving a weighed amount of sample with an aqueous HCl solution or were quantified on a JEOL JEM−3100F energy-filtering (Omega type) transmission electron microscope attached with energy dispersive X-ray spectrometer (EDS).

RESULTS AND DISCUSSION

A representative XRD pattern for the starting brucite hydroxide ($Co(OH)_2$, $Co_{1-x}Fe_x(OH)_2$ (x = $^1/_6$, $^1/_5$, $^1/_4$, $^1/_3$) and $Co^{2+}{}_{2/3}Ni^{2+}{}_{1/3}(OH)_2$) is shown in Figure 2. All the diffraction

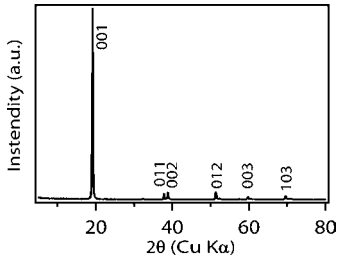

Figure 2. Typical XRD pattern of synthesized brucite hydroxide $Co_{3/4}Fe_{1/4}(OH)_2$.

peaks can be readily indexed in a hexagonal unit cell with lattice parameters of a ∼ 3.1 Å and c ∼ 4.6 Å. A basal spacing of ∼4.6 Å is characteristic of brucite-type phase without intercalated agents. Sharp reflections in the XRD pattern reveal a high crystallinity of the sample. Figure 3 shows representative SEM images of the as-prepared samples. The products typically consist of uniform hexagonal platelets with a mean lateral size of ∼2 μm and a thickness of approximately ∼100 nm. No impurity in other morphology was observed in the samples. The ratio of metallic contents (Co/Fe, Co/Ni) in the brucite-like product was quantified and found consistent with the designed molar ratio in the starting solution.

Taking $Co_{1-x}Fe_x(OH)_2$ as an example, the oxidative intercalation of $Co_{1-x}Fe_x(OH)_2$ is initiated from the oxidation of ferrous cations (Fe^{2+}) into ferric ones (Fe^{3+}), as a result of lower oxidation potential of Fe^{2+} in comparison with that of Co^{2+} ($Fe(OH)_2/Fe(OH)_3$, −0.58 V; $Co(OH)_2/Co(OH)_3$, 0.17 V), by donating electrons to iodine and simultaneous intercalation of *in situ* produced iodide (I_2/I^-, 0.535 V). The host layer charge or unit cell charge of resultant LDH product is determined by the ratio x.

$$Co^{2+}{}_{1-x}Fe^{2+}{}_x(OH)_2 + \frac{x}{2}I_2 \Leftrightarrow Co^{2+}{}_{1-x}Fe^{3+}{}_x(OH)_2I_x$$

When a stoichiometric amount of iodine was used, only $Co^{2+}{}_{2/3}Fe^{2+}{}_{1/3}(OH)_2$ (x = $^1/_3$ in $Co^{2+}{}_{1-x}Fe^{2+}{}_x(OH)_2$) was completely transformed into a pure LDH phase, characteristic with a basal spacing of ∼8.3 Å (8.3/4.15 Å series) (Figure 4a).

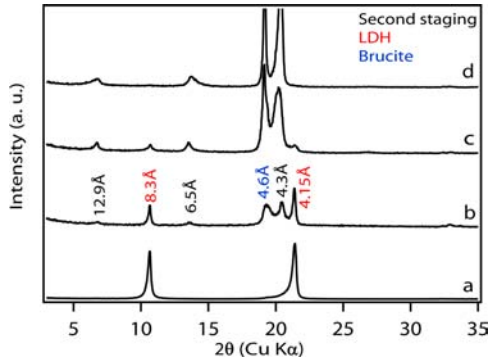

Figure 4. XRD patterns for the transformed products of 2 mmol $Co_{1-x}Fe_x(OH)_2$ (x = $^1/_3$, $^1/_4$, $^1/_5$, $^1/_6$) after treatment with stoichiometric iodine (x mmol I_2): (a) $Co_{2/3}Fe_{1/3}(OH)_2$ (x = $^1/_3$), (b) $Co_{3/4}Fe_{1/4}(OH)_2$ (x = $^1/_4$), (c) $Co_{4/5}Fe_{1/5}(OH)_2$ (x = $^1/_5$), (d) $Co_{5/6}Fe_{1/6}(OH)_2$ (x = $^1/_6$).

It indicates the formation of $Co_{2/3}{}^{2+}$−$Fe_{1/3}{}^{3+}$ LDH with an expanded iodide-intercalated gallery ∼8.3 Å (c'/3; LDH is a rhombohedral structure (c' ∼ 24.9 Å) in contrast with simple hexagonal brucite (c ∼ 4.6 Å)).[26,29] The same treatment on $Co^{2+}{}_{3/4}Fe^{2+}{}_{1/4}(OH)_2$, $Co^{2+}{}_{4/5}Fe^{2+}{}_{1/5}(OH)_2$, and $Co^{2+}{}_{5/6}Fe^{2+}{}_{1/6}(OH)_2$ (x = $^1/_4$, $^1/_5$, and $^1/_6$ in $Co^{2+}{}_{1-x}Fe^{2+}{}_x(OH)_2$) yielded mixed-phase products, namely I^--intercalated LDH (8.3/4.15 Å), a new series of basal spacing (12.9/6.5/4.3 Å) together with residual brucite (4.6 Å) (Figure 4b−d). The new spacing of 12.9 Å reveals the occurrence of second staging, corresponding to an alternated stacking of I^--

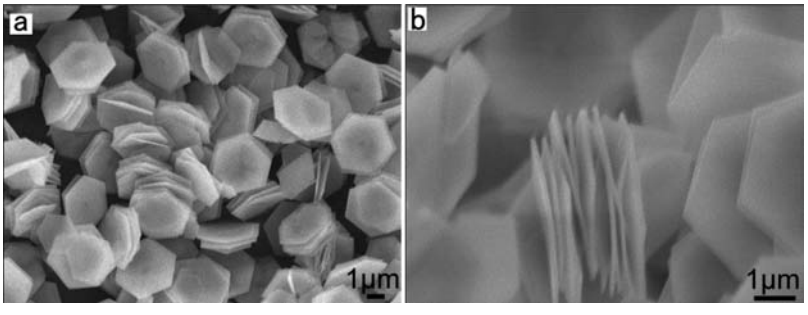

Figure 3. (a) Typical SEM images of as-synthesized uniform hexagonal platelets of brucite hydroxide $Co_{3/4}Fe_{1/4}(OH)_2$. (b) Some platelets are tilted and become nearly perpendicular, showing an estimated thickness of ∼100 nm.

intercalated slab (8.3 Å) and brucite slab (4.6 Å). Further carefully comparing the patterns, a notable difference is the absence of the reflection series of 8.3/4.15 Å for the product started from $Co^{2+}_{5/6}Fe^{2+}_{1/6}(OH)_2$ alone (Figure 4d). It implies that, for this particular composition, any I^--intercalated slab seems always adjacent with a brucite slab. In other words, there is no consecutive stacking of I^--intercalated slabs. These observations point toward a possible correlation between the Fe/Co ratio in the host sheets and I^--content in the interlayer gallery, producing different staging phenomena. In addition, residual brucite observed in $Co^{2+}_{1-x}Fe^{2+}_{x}(OH)_2$ with less Fe content ($x < {}^1/_3$) appears to be a possible result of kinetic oxidation condition arising from stoichiometric dose of iodine as well as crystallography positions of Fe^{2+} in starting brucite hydroxide deemed unfavorable for the oxidation into Fe^{3+}, which will be discussed later. Increasing the dose of iodine, which facilitates the kinetic oxidation of Fe^{2+}, will decrease the portion of residual brucite. However, it correspondingly increases the portion of LDH segment (8.3/4.15 Å) due to an enhanced opportunity for the oxidation of Co^{2+} rather than a sole oxidation of Fe^{2+}.[29] In practice, it proves very difficult to obtain a pure second-staging product from this reaction.

On the other hand, for pure $Co(OH)_2$ under stoichiometric treatment of iodine, there was no observation of any staging phenomena; instead there is a phase segregation or physical mixture of negligible LDH component (8.3/4.15 Å) and major unreacted brucite (4.6 Å) (see Figure 5a) due to insufficient

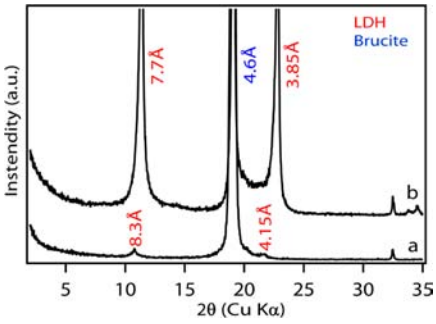

Figure 5. XRD patterns for the transformed products of 2 mmol $Co(OH)_2$ (a) after treatment with stoichiometric iodine ($^1/_3$ mol I_2), (b) after treatment with stoichiometric bromine ($^1/_3$ mol Br_2).

power of stoichiometric iodine for the oxidation of Co^{2+}. Furthermore, as shown in Figure 5b, there was no staging product observed for $Co(OH)_2$ under similar treatment of more powerful oxidizing bromine (Br_2/Br^-, 1.065 V) either, though the LDH segments intercalating bromide (7.7/3.85 Å) are significantly increased. The absence of a staging phase was also confirmed for $Co^{2+}_{2/3}Ni^{2+}_{1/3}(OH)_2$ in the reaction with bromine, affirming that LDH phase evolution is again associated with different metallic composition/ratio in starting brucite hydroxides.

The above experimental results concerning possible stacking sequence and phase segregation may be summarized by a schematic model shown in Figure 6. The lowest limit of host layer charge to prop up a hydroxide gallery is generally taken as $^1/_5$,[42] approximately about 20% oxidation of M^{2+} into M^{3+}, and there were various reports on coprecipitated LDH products with M^{3+}/M^{2+} ratio between $^1/_5$ and $^1/_3$.[3] However, for the current topochemical synthesis, the experimental evidence seem not supporting the formation of pure LDH products with

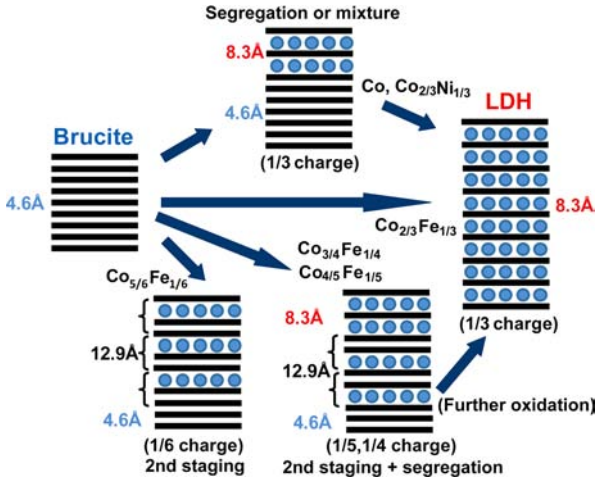

Figure 6. Proposed model for different staging products and phase segregation correlating with the metallic composition/ratio or host layer charge.

any host layer charge lower than $^1/_3$ (33% oxidation of M^{2+} into M^{3+}).

As already mentioned above in Figure 1, the topochemical transformation from brucite into LDH would likely involve a rapid oxidation of outermost M^{2+} edge sites with an inward advance of oxidation front and charge propagation within the brucite sheet. The charge propagation may be realized by charge transfer or valence interchange between adjacent donor and acceptor sites, i.e., electron or hole hopping. Generally, hopping model is regarded suitable when there are valence-variable ions (transition-metal cations here), and the ions with different valences locate at the same crystallographic position (all sites are equivalent in the brucite sheet). If an M^{2+} is oxidized into M^{3+}, a valence interchange reaction, between adjacent M^{2+} and M^{3+} sites, which are connected by hydroxyl (oxygen) bridges, should be possible. In this viewpoint, for any outermost M^{2+} site that is oxidized into M^{3+} via electron transfer to halogen agents, the site can be reduced back to M^{2+} by accepting an electron from adjacent M^{2+} sites and relaying the hole through the lattice away from the particular site. This provides a reasonable mechanism for restoration of electron donor sites at the interface between brucite crystallites and halogen agents for a continual reaction.

The study on green rust $(Fe^{2+}_2Fe^{3+}(OH)_6A^{n-}_{1/n})$[42−45] has demonstrated that the connectivity and crystallographic bonding geometry between the donor and the acceptor cations have a strong influence on the electron hopping mobility. The charge hopping or replenish process is supposed to be strongly directional, with much greater tendency to operate along basal directions within the sheets than across the interlayer gallery. The Hartree−Fock calculations of the Fe^{2+}−Fe^{3+} valence interchange rates show that, among different iron-to-iron hops in basal directions within a white rust ($Fe(OH)_2$) sheet, a hop to next-nearest neighbors at an intermediate distance is the fastest. The predicted hopping rate is on the order of 10^{10} s^{-1} (at 300 K), whereas all other possibilities, including those to the first ring of six nearest neighboring sites surrounding the transient Fe^{3+} site, are predicted to be slower than 10^3 s^{-1}.[46] In the current case, the crystallography feature of starting brucite and corresponding LDH are very similar to that of white rust and corresponding green rust. Therefore, high electron mobility in the host sheet, allowing long-range charge transport, would

dx.doi.org/10.1021/ja310246r | J. Am. Chem. Soc. 2012, 134, 19915−19921

be considered as the prerequisite for the oxidative intercalation transformation to proceed. Different metallic composition and ratio, which actually determine attainable host layer charge and affect hopping rate as well, would fundamentally impact the reaction kinetics.

Accompanying the propagation of positive electrical charge in the host sheets, reduced halide anions are intercalated and diffused into the gallery. The intercalation of halide will increase the repulsion between neighboring galleries because of the relatively small thickness of the hydroxide layer, which might increase the probability in forming a staging product with alternated stacking of filled and empty galleries; i.e., adjacent galleries are not opened when host layer charge is compensated within one gallery. In comparison with graphite intercalation where the facile sheet flexibility allows for buckling of layers on edge opening at different intercalations sites by creating localized domain islands of guest occupancy, the proposed model for staging phase in LDH system usually excludes buckling of layers given the inherent rigid nature.[32,35,37] No further high-order staging besides the second-order one was observed in the current study, similar to previous cases of LDH system. This may hint that relatively few edge nucleation sites spread along the edges rapidly in an ordered manner; i.e., the initial edge opening rate might be accelerated when there are adjacent (or nearly adjacent) expanded galleries. On the other hand, the intersheet charge transfer across the gallery may also facilitate the reaction in a progressive manner. The intersheet hopping through vacuum is predicted to be extremely slow (10^{-8} s^{-1} at 300 K).[46] However, the interlayer constituents may provide a plausible means for increasing the electronic interaction across the gallery. During the topochemical transformation, we expect that intercalated halide anions and water molecules might offer a structural configuration for increasing the rate of charge hopping to an adjacent sheet, which is supposed to be helpful in forming a pure LDH phase. Such a counter balance appears to be the driving mechanism for the transformation into either pure LDH or staging product dependent on the reaction conditions.

On the basis of the above assumptions, plausible charge propagation paths are schematically drawn in Figure 7. It can be seen from the schematic model that a hopping to next-nearest neighbors at an intermediate distance of $\sqrt{3}a$ (5.37 Å, red arrows) in fact produces a most preferable propagation path for the development and distribution of charge centers M^{3+}. If all the charge hopping occurs in the fastest rate, a supercell containing two M^{2+} sites and one M^{3+} sites is naturally achieved, without direct nearest neighboring of charge center M^{3+} (Figure 7b). As a precondition, it is reasonable to assume that, in a heterometallic (Co/Fe) brucite-type hydroxide, the divalent metal cations will orderly distribute in the host sheet following their molar fraction. Such an ordering may be derived from the size, bonding nature, or spin state of different cations. That is to say that a corresponding supercell containing one Fe cation and $(1 - x)/x$ Co cations ($x = {}^1/_3$, ${}^1/_6$) would be expected. As a result, a pure phase of Co^{2+}–Fe^{3+} LDH, which occurs in $x = {}^1/_3$ case (Figure 4a), coincides with the assumption that one Fe^{3+} and two Co^{2+} are neatly ordered in a supercell, achieving the highest host layer charge (all Fe^{2+} are oxidized) while avoiding direct nearest neighboring of Fe^{3+}. As the electron transport in the host sheet would be concurred with the diffusion of iodide anion in the interlayer gallery, each oxidized Fe^{3+} will produce one anionic site in the interlayer gallery. Each intercalated iodide anion will share/balance its charge with one Fe^{3+} cation in the layer above and/or underneath, representing a uniform intercalation of iodide (one per supercell) in the gallery. Therefore, a supercell containing one positive electric charge will be balanced by a spherical iodide separated by a distance of $\sqrt{3}a$ (5.37 Å), commensurate with the cationic ordering in the host layer.[29] It is the most ideal scenario for effectively separating apart host sheets and achieving a complete phase transformation from brucite into pure LDH.

For $x = {}^1/_6$ case, in comparison with $x = {}^1/_3$, only half of sites locating along the fastest hopping routes are occupied by Fe^{2+} cations, whereas the other half would be Co^{2+} cations, which may act as relaying points for charge propagation. Co^{2+} at these relaying sites may be transiently oxidized into Co^{3+} and eventually reduced back to Co^{2+} by diffusion of the hole to available Fe^{2+} sites (see Figure 7c). All sites participating in a charge transport process, permanent or transient, still locate along the fastest hopping directions, and the reaction is thus supposed to be not significantly different from the case of $x = {}^1/_3$. Nevertheless, for a host layer charge of ${}^1/_6$, two adjacent layers yield a combined charge sum of ${}^1/_6 + {}^1/_6 = {}^1/_3$. This means that overall host layer charge, the layer above and underneath, may be completely saturated/canceled out by intercalating an iodide per supercell in the gallery. No intercalation would be expected to occur in the directly adjacent gallery (see schematic model $Co_{5/6}Fe_{1/5}$ in Figure 6). This inevitably produces an ordered stacking of LDH slabs (iodide-intercalated gallery) and brucite (empty gallery) resulting in a basal spacing of 12.9 Å, whereas no consecutive stacking of LDH component (8.3 Å) would be possible. It thus well explains the XRD results on the second staging product started from $Co^{2+}{}_{5/6}Fe^{2+}{}_{1/6}(OH)_2$ with the absence of 8.3 Å reflection peak in Figure 4d.

For other intermediate compositions of $x = {}^1/_4$, ${}^1/_5$ falling between the two boundaries of lowest ${}^1/_6$ and highest ${}^1/_3$, the charge propagation has to involve the hopping to direct nearest neighboring sites at a cation–cation distance of ~3.1 Å (gray arrows in Figure 8a,b) if similar supercells containing one Fe cation and $(1 - x)/x$ Co cations ($x = {}^1/_4$, ${}^1/_5$) are presumed. As a consequence, some Fe^{2+} might not be readily oxidized into Fe^{3+} as they are not sitting on the fastest charge propagation sites. This raises the possibility for the presence of Co^{3+} due to aforementioned required symmetry in the fastest charge distribution. It actually brings up a dilemma of whether to exactly follow the fastest charge propagation path (partially

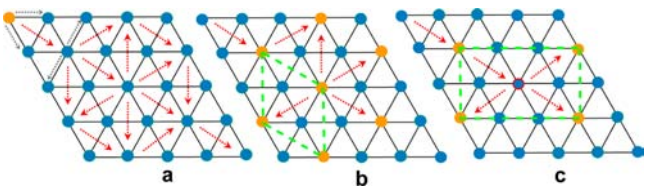

Figure 7. (a) Plausible edge-inward charge propagation directions from outermost edge site in a brucite sheet. Red arrows represent most preferable next-nearest neighboring hopping whereas gray arrows indicate less favorable nearest neighboring ones. (b) Charge propagation along the fastest next-nearest neighboring hopping to attain host layer charge of ${}^1/_3$. (c) Charge propagation to attain host layer charge of ${}^1/_6$. Green dashed lines in parts b and c enclose a supercell containing one positive electric charge. The locations of M^{3+} (orange spheres) are based on an ordered distribution of Fe cations in $Co_{1-x}Fe_x(OH)_2$ ($x = {}^1/_3$, ${}^1/_6$).

dx.doi.org/10.1021/ja310246r | J. Am. Chem. Soc. 2012, 134, 19915–19921

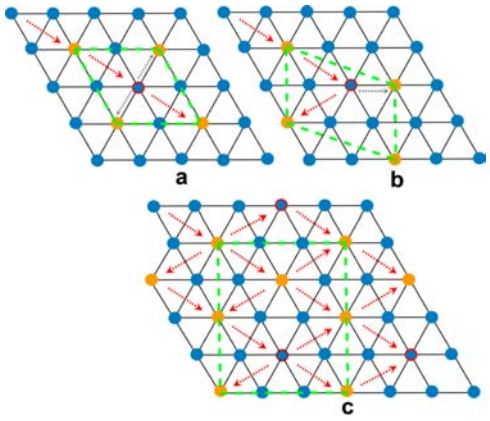

Figure 8. Plausible charge propagation route to attain (a) $^1/_4$ host layer charge, and (b) $^1/_5$ host layer charge based on forming uniform supercells in $Co_{1-x}Fe_x(OH)_2$ ($x = {}^1/_4, {}^1/_5$). (c) Alternative intergrowth model of two $^1/_3$ and one $^1/_6$ supercells to yield a combined three electric charge as 12 cations in total are counted (green dashed lines), i.e., a nominal layer charge of $^1/_4$. The labels are the same with those in Figure 7.

producing Co^{3+}) or to exactly reflect the lower oxidation potential of Fe^{2+} in comparison with Co^{2+} (only yielding Fe^{3+}). The phase transformation is therefore somewhat complicated and does not necessarily straightforwardly reflect the Fe/Co ratio in starting brucite hydroxides. An alternative interpretation is that an intergrowth of supercells as described in Figure 7b ($x = {}^1/_3$) and Figure 7c ($x = {}^1/_6$), might yield host sheets with nominal composition of $x = {}^1/_4$ and $^1/_5$. During the topochemical transformation, these intergrown supecells might be directly evolved into mosaic domains with host layer charge of $^1/_3$ or $^1/_6$, respectively. Figure 8c illustrates an example for the possible intergrowth of two $^1/_3$ and one $^1/_6$ supercells to yield a combined three positive electric charge as 12 cations in total are counted, i.e., $^1/_4$ layer charge. In other words, the charge propagation in the host sheet, accordingly the anion diffusion in the gallery, may be regarded as a mosaic effect of the above scenarios already discussed for $x = {}^1/_3$ and $^1/_6$ cases. As a result, LDH segment (8.3 Å) as well as second staging product of LDH and brucite (12.9 Å) are both likely formed in the transformed product from starting nominal compositions of $x = {}^1/_4$ and $^1/_5$, consistent with the XRD observations in Figure 4.

When excessive oxidizing agents are supplied, it creates the capacity of oxidizing Co^{2+} to Co^{3+}, in addition to a sole oxidation of Fe^{2+}, to attain an overall layer charge of $^1/_3$ in all host sheets regardless the Fe/Co ratio. In fact, wet chemical analyses also determined that host layer charge in all as-transformed single LDH phase was invariably close to $^1/_3$. This evidence strongly supports that some Co^{2+} may be oxidized into Co^{3+} if the Fe^{3+} content alone cannot reach the $^1/_3$ charge threshold, e.g., in $Co_{4/5}Fe_{1/5}$ or $Co_{3/4}Fe_{1/4}$ under further oxidation (Figure 6). Accordingly, a fully developed host layer charge of $^1/_3$ may be taken as the general requirement to form a single LDH phase in the current oxidative intercalation reaction.

Then the remaining question turns to why staging phenomena were not observed for monometallic $Co(OH)_2$ and bimetallic $Co_{2/3}Ni_{1/3}(OH)_2$ in the same transformation. Unlike $Co_{1-x}Fe_x(OH)_2$ ($x = {}^1/_6, {}^1/_5, {}^1/_4$) which needs hetero-oxidation of both Fe^{2+} and Co^{2+} to reach an ideal layer charge of $^1/_3$, and therefore the reaction may be somewhat sluggish, the transformation of $Co(OH)_2$ and bimetallic $Co_{2/3}Ni_{1/3}(OH)_2$ into LDHs is dependent on sole oxidation of Co^{2+} into Co^{3+}. In both $Co(OH)_2$ and bimetallic $Co_{2/3}Ni_{1/3}(OH)_2$, there are sufficient Co^{2+} sites sitting on the favorable charge propagation route to attain the highest layer charge of $^1/_3$. It also implies that once the oxidation of an outermost edge Co^{2+} site is initiated, the reaction and positive electric charge would probably propagate along the fastest hopping directions (Figure 7b), always attaining an ideal charge of $^1/_3$ in the host sheet and simultaneous to a full intercalation of anions, similar to the case on $Co_{2/3}Fe_{1/3}(OH)_2$ with a sole oxidation of Fe^{2+} into Fe^{3+}. The reaction may be expressed as

$$Co^{2+}(OH)_2 + \frac{1}{6}A_2 \Leftrightarrow {Co^{2+}}_{2/3}{Co^{3+}}_{1/3}(OH)_2A_{1/3}$$

(A = I, Br)

As a result, every host layer charge is perfectly balanced/saturated by the halide anions diffused above/beneath. If the oxidation potential of halogen agent is not high enough or the dose is not sufficient, it results in some portion of transformed LDH (with an ideal layer charge of $^1/_3$) and residual brucite (Figure 5b). Once the dose of oxidizing halogen agent is sufficient and the reaction kinetics is ensured (i.e., extended reaction time), a single LDH phase is attainable.[27,28]

From the above discussion, it can be seen that the topochemical transformation from brucite to LDH appears to strongly support a reasonable assumption for a charged host sheet: no direct nearest neighboring of M^{3+}–M^{3+}, which echoes the discussion on cation ordering in LDH structure in literature.[39,40] On the basis of such a principle, a host layer charge of $^1/_3$ (i.e., M^{2+}/M^{3+} = 2:1) is the most ideal condition for the formation of a most stable LDH structure. Though conventional coprecipitation procedure claimed the preparation of LDH with M^{2+}/M^{3+} ratio other than 2, the possibility is high that the microscopic structure would be mosaic domain islands of both brucite (neutral) and LDH with M^{2+}/M^{3+} ratios of 2, producing a nominal layer charge lower than $^1/_3$. On the other hand, the current topochemical transformation, similar to homogeneous precipitation, might be very difficult, if it is not impossible, in obtaining a single LDH phase with a host layer charge lower than $^1/_3$. This may be ascribed to a more thermodynamic equilibrated condition for both topochemical transformation and homogeneous precipitation than that of conventional coprecipitation, which precludes the formation of mosaic domains in LDH host sheets. The underlying aspects revealed in this topochemical transformation therefore provide new insights into structure evolution of general LDH structure, particularly concerning host layer charge, M^{2+}/M^{3+} cation arrangement, and phase evolution.

It is also worth adding that the understanding of charge transport or valence interchange in LDH may be important for some practical applications. Since charge transport in a redoxable transition-metal brucite/LDH sheet seems facile, it raises the prospect of transferring electrons (charges) out of hydroxide sheets, which might be essential in utilizing them as active materials for electrochemical energy storage or adsorption/degradation of redox-active contaminant species for environmental purpose, etc.

■ CONCLUSIONS

In summary, the topochemical transformation from brucite ($Co_{1-x}Fe_x(OH)_2$, $Co(OH)_2$, ${Co^{2+}}_{1-x}{Ni^{2+}}_x(OH)_2$) to corre-

sponding LDHs under halogen agents (iodine, bromine) seems not to be able to produce a single LDH phase with any host layer charge lower than $^1/_3$, in stark contrast with conventional coprecipitation process. Especially, for $Co_{1-x}Fe_x(OH)_2$ ($x = {}^1/_6$, $^1/_5$, $^1/_4$), second staging products were observed. On the other hand, for pure $Co(OH)_2$ or $Co^{2+}{}_{1-x}Ni^{2+}{}_x(OH)_2$, there was no observation of staging phenomena, instead a phase segregation or physical mixture for any unfulfilled transformation. On the basis of a plausible charge (electron, hole) hopping scenario in brucite sheets, the metallic composition/ratio actually determines the attainable layer charge and also affects charge hopping rate, fundamentally impacting the reaction kinetics. A correlation between the metallic composition/ratio in the host sheets and anion content in the interlayer gallery was proposed to well explain the phase evolution observed. The study helps to develop an in-depth understanding of this important topochemical reaction and redox behavior in transition-metal hydroxides. It also sheds light on some important structural aspects of LDHs in general, e.g., precise composition control, host layer charge, phase evolution, etc. Among them, no direct nearest neighboring of M^{3+}–M^{3+} charge centers in host sheets under equilibrium conditions seems to be affirmed as one of the most important principles governing the formation of a stable and pure LDH structure. This work therefore not only illustrates the underlying aspects for the topochemical transformation itself, but also presents new insights into structural evolution of LDH, particularly a clear understanding of host layer charge, cation ratio, and cation ordering.

AUTHOR INFORMATION

Corresponding Author

MA.Renzhi@nims.go.jp

Notes

The authors declare no competing financial interest.

ACKNOWLEDGMENTS

This work was partly supported by the World Premier International Research Center (WPI) initiative on Materials Nanoarchitectonics, MEXT, Japan, and CREST of the Japan Science and Technology Agency (JST). R.M. acknowledges the support from JSPS KAKENHI Grant Number 24310095.

REFERENCES

(1) Allmann, R. *Acta Crystallogr., Sect. B* **1968**, *24*, 972.
(2) Braterman, P. S.; Xu, Z. P.; Yarberry, F. In *Layered Double Hydroxides (LDHs), Handbook of Layered Materials*; Auerbach, S. M., Carrado, K. A., Dutta, P. K., Eds.; Marcel Decker, Inc.: New York, 2004; pp 373–474.
(3) Rives, V. *Layered Double Hydroxides: Present and Future*; Nova Science Publishers, Inc.: New York, 2006.
(4) Duan, X.; Evans, D. G. *Layered Double Hydroxides, Structure and Bonding Series*; Springer-Verlag: Berlin, 2006.
(5) Cavani, F.; Trifirò, F.; Vaccari, A. *Catal. Today* **1991**, *11*, 173.
(6) Sels, B.; De Vos, D.; Buntinx, M.; Pierard, F.; Kirsch-De Mesmaeker, A.; Jacobs, P. *Nature* **1999**, *400*, 855.
(7) Sels, B. F.; De Vos, D. E.; Jacobs, P. A. *Catal. Rev* **2001**, *43*, 443.
(8) Liu, Z.; Ma, R.; Osada, M.; Takada, K.; Sasaki, T. *J. Am. Chem. Soc.* **2005**, *127*, 13869.
(9) Liu, X.; Ma, R.; Bando, Y.; Sasaki, T. *Angew. Chem., Int. Ed.* **2010**, *49*, 8253.
(10) Liu, X.; Ma, R.; Bando, Y.; Sasaki, T. *Adv. Mater.* **2012**, *24*, 2148.
(11) Ma, R.; Liu, Z.; Li, L.; Iyi, N.; Sasaki, T. *J. Mater. Chem.* **2006**, *16*, 3809.
(12) Ma, R.; Sasaki, T. *Adv. Mater.* **2010**, *22*, 5082.
(13) Ma, R.; Sasaki, T. *Recent Pat. Nanotechnol.* **2012**, *6*, 159.
(14) Reichle, W. T. *Solid State Ionics* **1986**, *22*, 135.
(15) Ehlsissen, K. T.; Delahaye-Vidal, A.; Genin, P.; Figlarz, M.; Willmann, P. *J. Mater. Chem.* **1993**, *3*, 883.
(16) Xu, R.; Zeng, H. C. *Chem. Mater.* **2001**, *13*, 297.
(17) Caravaggio, G. A.; Detellier, C.; Wronski, Z. *J. Mater. Chem.* **2001**, *11*, 912.
(18) Cai, H.; Hillier, A. C.; Franklin, K. R.; Nunn, C. C.; Ward, M. D. *Science* **1994**, *266*, 1551.
(19) Costantino, U.; Marmottini, F.; Nocchetti, M.; Vivani, R. *Eur. J. Inorg. Chem.* **1998**, *10*, 1439.
(20) Costantino, U.; Coletti, N.; Nocchetti, M.; Aloisi, G. G.; Elisei, F.; Latterini, L. *Langmuir* **2000**, *16*, 10351.
(21) Ogawa, M.; Kaiho, H. *Langmuir* **2002**, *18*, 4240.
(22) Liu, Z.; Ma, R.; Osada, M.; Iyi, N.; Ebina, Y.; Takada, K.; Sasaki, T. *J. Am. Chem. Soc.* **2006**, *128*, 4872.
(23) Liu, Z.; Ma, R.; Ebina, Y.; Iyi, N.; Takada, K.; Sasaki, T. *Langmuir* **2007**, *23*, 861.
(24) Iyi, N.; Matsumoto, T.; Kaneko, Y.; Kitamura, K. *Chem. Lett.* **2004**, *33*, 1122.
(25) Li, L.; Ma, R.; Ebina, Y.; Iyi, N.; Sasaki, T. *Chem. Mater.* **2005**, *17*, 4386.
(26) Ma, R.; Liu, Z.; Takada, K.; Iyi, N.; Bando, Y.; Sasaki, T. *J. Am. Chem. Soc.* **2007**, *129*, 5257.
(27) Ma, R.; Takada, K.; Fukuda, K.; Iyi, N.; Bando, Y.; Sasaki, T. *Angew. Chem., Int. Ed.* **2008**, *47*, 86.
(28) Liang, J.; Ma, R.; Iyi, N.; Ebina, Y.; Takada, K.; Sasaki, T. *Chem. Mater.* **2010**, *22*, 371.
(29) Ma, R.; Liang, J.; Takada., K.; Sasaki, T. *J. Am. Chem. Soc.* **2011**, *133*, 613.
(30) Rüdorff, W. *Chimia* **1965**, *19*, 489.
(31) Herold, A. *Synth. Met.* **1988**, *23*, 27.
(32) Fogg, A. M.; Dunn, J. S.; O'Hare, D. *Chem. Mater.* **1998**, *10*, 356.
(33) Pisson, J.; Taviot-Guého, C.; Israëli, Y.; Leroux, F.; Munsch, P.; Itié, J.-P.; Briois, V.; Morel-Desrosiers, N.; Besse, J.-P. *J. Phys. Chem. B* **2003**, *107*, 9243.
(34) Feng, Y.-J.; Williams, G. R.; Leroux, F.; Taviot-Gueho, C.; O'Hare, D. *Chem. Mater.* **2006**, *18*, 4312.
(35) Williams, G. R.; Fogg, A. M.; Sloan, J.; Taviot-Guého, C.; O'Hare, D. *Dalton Trans.* **2007**, 3499.
(36) Iyi, N.; Kurashima, K.; Fujita, T. *Chem. Mater.* **2002**, *14*, 583.
(37) Ma, S.; Fan, C.; Du, L.; Huang, G.; Yang, X.; Tang, W.; Makita, Y.; Ooi, K. *Chem. Mater.* **2009**, *21*, 3602.
(38) Taviot-Guého, C.; Feng, Y.; Faour, A.; Leroux, F. *Dalton Trans.* **2010**, *39*, 5994.
(39) Belloto, M.; Rebours, B.; Clause, O.; Lynch, J.; Elkaïm, E. *J. Phys. Chem.* **1996**, *100*, 8527.
(40) Sideris, P. J.; Nielsen, U. G.; Gan, Z.; Grey, C. P. *Science* **2008**, *321*, 113.
(41) Jobbágy, M.; Iyi, N. *J. Phys. Chem. C* **2010**, *114*, 18153.
(42) Génin, J.-M. R.; Ruby, C. *Solid State Sci.* **2004**, *6*, 705.
(43) Cuttler, A. H.; Man, V.; Cranshaw, T. E.; Longworth, G. *Clay Miner.* **1990**, *25*, 289.
(44) Refait, Ph.; Abdelmoula, M.; Génin, J.-M. R. *Corros. Sci.* **1998**, *40*, 1547.
(45) Génin, J.-M. R.; Bourrié, G.; Trolard, F.; Abdelmoula, M.; Jaffrezic, A.; Refait, P.; Maitre, V.; Humbert, B.; Herbillon, A. *Environ. Sci. Technol.* **1998**, *32*, 1058.
(46) Wander, M. C. F.; Rosso, K. M.; Schoonen, M. A. A. *J. Phys. Chem. C* **2007**, *111*, 11414.